Available online at www.sciencedirect.com

ScienceDirect

Procedia CIRP 111 (2022) 605–608

www.elsevier.com/locate/procedia

12th CIRP Conference on Photonic Technologies [LANE 2022], 4-8 September 2022, Fürth, Germany

Patterning of WOx, VOx, and MoOx thin-films with picosecond and nanosecond laser sources

C. Munoz-Garcia [a,*], D. Canteli [a], S. Lauzurica[a], M. Morales[a], C. Molpeceres[a], Eloi Ros[b], P. Ortega[b], J.M. López-González[b], C. Voz[b]

[a]*Centro Láser. Universidad Politécnica de Madrid (UPM). C/ Alan Turing 1, 28031, Madrid, Spain*
[b]*Universitat Politecnica de Catalunya (UPC) C/ Jordi Girona 1-3, 08034, Barcelona, Spain*

* Corresponding author. Tel.: +34 91 067 87 85. *E-mail address:* cristina.munozg@upm.es

Abstract

Transition metal oxide (TMOs) layers have interesting properties as selective contacts, i.e., hole or electron transport layers for novel semiconductor devices. Especially, oxides of molybdenum (MoO_3), vanadium (V_2O_5), and tungsten (WO_3) show good bahaviour acting as front hole-selective contacts for n-type crystalline-silicon heterojunction solar cells. Laser scribing has been widely used for thin-film ablation and seems the appropriate technology for device manufacturing with such non-conventional materials. In this work, we study the laser scribing of non-stoichiometric evaporated WO_x, VO_x, and MoO_x films with three different wavelengths (1064, 532, and 355 nm) with pulse duration in the nanosecond and picosecond regimes. The selection of the proper laser source allows a wide parametric window, with complete removal of the TMO films and no alteration of the silicon substrate. The results on the isolation of diodes and their electrical characteristics show the quality of the laser scribing processes.

Keywords: Transition metal oxides (TMO), hole transport layer, selective contacts, silicon solar cells, laser ablation, fluence threshold

1. Introduction

Silicon heterojunction (SHJ) devices were conceived and developed as a way to increase the efficiency of first-generation silicon solar cells by the use of thin layers of hydrogenated amorphous silicon (a: Si-H) deposited on crystalline silicon (c-Si) wafers. The advantage of this technology is that it can be carried out at a low temperature, but the heterojunction emitters present a high sheet resistance [1]. To improve efficiency, different technologies have been proposed such as Heterojunction with Intrinsic Thin Layer [2][3], or Tunnel Oxide Passivated Contact [4].

Another alternative is the use of Transition Metal Oxides (TMOs) as hole or electron transport layers (HTL or ETL, respectively). These layers are known as selective contacts and can be deposited on both electrodes of a solar cell by simple fabrication routes. In this context, three transition metal oxides: molybdenum oxide (MoO_3), vanadium oxide (V_2O_5), and tungsten oxide (WO_3), have been analyzed as front hole-selective contacts for n-type crystalline silicon heterojunction solar cells [5] [6] [7]. The most significant feature of thermally evaporated non-stoichiometric MoO_x, VO_x, and WO_x films is their high work function, up to 6.9 eV, much higher than that of elemental metals. Due to their high working function and wide energy band gaps (E_{gap}>3 eV), these oxides act as transparent hole-selective contacts with semiconductive properties that are determined by oxygen vacancy defects [8].

Laser scribing can be described in a general way as the irradiation of the material surface, leading to the heating, melting, and evaporation of the material. To have a full image of the laser scribing of thin films, we should analyze

10.1016/j.procir.2022.08.160

the two principal parameters in the process: First, an adequate selection of the laser wavelength is going to affect not only the process efficiency but also the possibility to perform a selective removing of the top layer, depending on the absorption coefficients of the top layer and substrate [9]. Second, the laser pulse fluence is a key parameter to remove the top layer without affecting the substrate below. Of course, an adequate pulse repetition frequency and pulse overlap are necessary if more than a single pulse is required to process the target area [11]. We can define the damage fluence threshold as the minimum energy density needed to induce visible damage in the film [12]. And the same description can be used to define the fluence threshold for the oxide film removal, and for the presence of damage in the silicon substrate, being the process parametric window the difference between the latter two thresholds. In this work, we study the laser scribing process for three transition metal oxides, WO_x, VO_x, and MoO_x, of great interest because of their application as HTL layers on silicon. The main aim of this paper is to study the interaction between laser pulses of different wavelengths and pulse duration with films of these oxides deposited by evaporation.

2. Material and methods

2.1. Sample preparation

Three different oxide thin-films -MoO_x, VO_x, and WO_x- were deposited on crystalline silicon substrates to study the laser ablation process. Polished n-type Si wafers were dipped in dilute hydrofluoric acid (1%) to remove any native silicon oxide from their surface. Then, the different TMO layers were thermally sublimated in a vacuum ($<10^{-5}$ mbar) from a tantalum boat using high-quality powdered V_2O_5, MoO_3, and WO_3 precursors (Sigma Aldrich, > 99.99% purity). The deposition rate was regulated at around 0.2 Å/s with a quartz micro-balance for a total thickness of approximately 50 nm. The thin layers were grown on the substrates at room temperature and present a sub-oxidized composition, which is positive for the hole-selective behaviour.

2.2. Laser systems

Laser ablation experiments in these samples are carried out in the nanosecond and picosecond regimes with three wavelengths using different laser sources: For nanosecond pulses Nd: YVO4 DPSS sources emitting at 355 nm (HIPPO, Spectra-Physics), at 532 nm (Explorer, from Spectra-Physics), and at 1064 nm (Yb-fiber laser RFL-P20QE). In the picosecond range an Nd: YVO4 DPSS laser source (Lumera Super Rapid –HE) emitting at 355 nm, 532 nm, and 1064 nm was used. All laser sources work at TEM00 mode.

2.3. Ablation thresholds calculation. Measurement and characterization techniques

In laser ablation processes, it is important to determine appropriate energy density values that lead to effective material removal with minimum side effects. To establish the parametric windows, it is important to know the ablation thresholds. These thresholds can be easily measured from the relation between pulse fluence and crater diameter generated in the sample. [12].

$$D^2 = 2 \cdot w_0^2 ln\left[\frac{\phi_0}{\phi_{th}}\right] \quad (1)$$

Ablation-profile measurements and morphological characterization have been made using a confocal microscope (Sensofar, PL µ2300).

After that, the viability of this process has been evaluated by performing the optimized laser ablation steps to pattern devices based on these transition metal oxides. In particular, we isolated diodes fabricated on n-type c-Si with a reference ohmic contact of doped amorphous silicon on the rear side (cathode). On the front side (anode), the different oxides were used as hole-selective contacts with a metallic electrode consisting of a thin nickel layer (10 nm) of high work function capped by an aluminum layer (200 nm) for easier electrical characterization. The current-voltage characteristics were measured through a high-precision Keithley 2601B Source-Meter.

3. Results and discussion

In all samples, after the ablation process, the confocal microscopy shows that nanosecond pulses at 355 nm and 532 nm induce a good morphology with a clean edge (see figure 1). Nanosecond pulses lead to more melted and redeposited material, especially at 1064 nm, while picosecond pulses show a wider thermal affected zone, maybe due to the higher beam radius of the ps laser source.

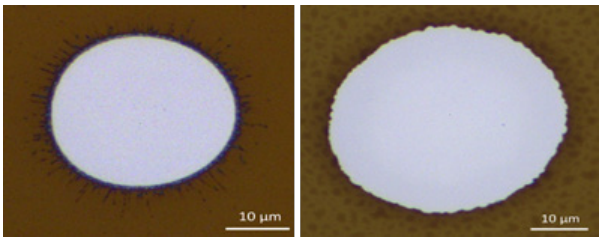

Fig. 1. Confocal microscope images of MoOx craters obtained with an 8 µJ nanosecond pulse (left) and picosecond pulse (right) at 532 nm.

To calculate the corresponding fluence thresholds, figure 2 shows an example of the relation between the square of the crater diameter and the logarithm of applied maximum laser pulse fluence (ϕ_0). In all oxides, the behaviour is the same. A well-defined linear dependence in a semi-log plot allows the calculation of the beam radius (ω_0). For each laser source, the obtained ω_0 values are independent of the evaluated oxide. An average value of the different ω_0 values obtained for the three oxides has been used for the fluence calculations.

With the nanosecond lasers, the obtained beam radius (ω_0) values are 18.7 ± 0.7 µm, 14.2 ± 0.8 µm, and 20.6 ± 0.1 µm for 355 nm, 532 nm, and 1064 nm wavelength, respectively. For picoseconds pulses, the beam radius is higher in all cases. The obtained values are 33.1 ± 0.5 µm (at 355 nm), 42.2 ± 0.8 µm (at 532 nm) and 62 ± 1 µm (at 1064 nm).

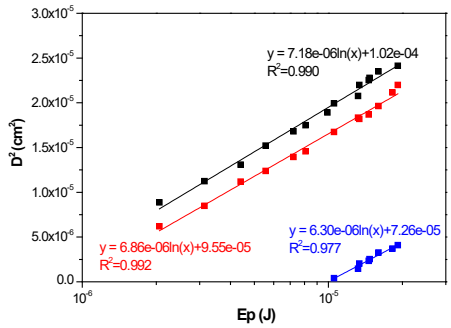

Fig. 2. For the ns pulsed regime at 355 nm of wavelength, the squared diameter of laser-induced damage crater of WOx films was plotted against applied pulse energy. (Black line -damage in the oxide film-, red line -total removal of the film- and blue line -substrate damage-).

Figure 3 and figure 4 show the threshold fluence values for the ns and ps regimes at the different wavelengths for the three oxides. Considering ns pulses, a given wavelength leads to very similar threshold fluences to remove the three different oxides (red columns Figure 3): 0.15 ± 0.02 J/cm^2 for 355 nm, 0.34 ± 0.08 J/cm^2 for 532 nm, and 4.9 ± 0.4 J/cm^2 for 1064 nm. The ablation threshold obtained at 1064 nm is more than one order of magnitude higher than that of other wavelengths, probably due to the longer pulse duration (120 ns at 1064 nm versus 12 ns and 15 ns at 355 nm and 532 nm, respectively), allowing a higher thermal diffusion of the absorbed energy into the material, so more power is needed to reach the melting temperature.

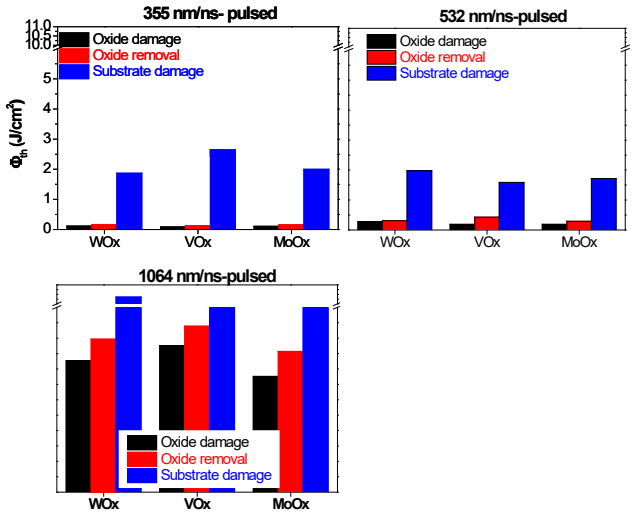

Fig. 3. Threshold fluence for the three oxides studied in this work in nanoseconds pulses at different wavelengths.

On the other hand, for the IR wavelength ps pulsed laser, no substrate damage is detected in any of the oxides studied. Moreover, in the particular case of VO_x working at 532 nm no silicon damage is detected either. Hence, the fluence thresholds for oxide removal obtained are 0.06 ± 0.02 J/cm^2 for 355 nm, 0.16 ± 0.02 J/cm^2 for 532 nm and 0.63 ± 0.11 J/cm^2 for 1064 nm. These values are lower than those obtained for ns pulses due to the shorter duration of the pulses -8ps in all wavelengths-. A longer laser pulse allows a higher thermal diffusion into the material, it needed more energy to remove the oxide layer.

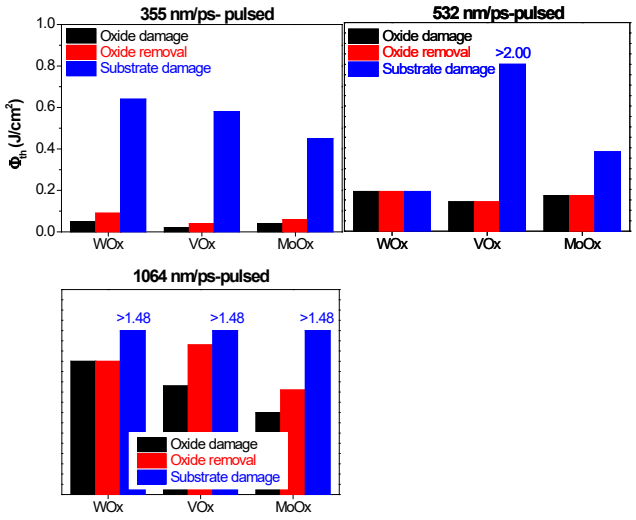

Fig. 4. Threshold fluence for the three oxides studied in this work in picoseconds pulses at different wavelengths.

Table 2 shows the average values of the parametric windows of the three studied oxides for each wavelength used in the ns and ps laser pulses. In the nanosecond regime, the parametric windows between oxide removal and substrate damage are about 2.0 J/cm^2 for 355 nm, 1.5 J/cm^2 for 532 nm, and about 5.5 J/cm^2 for 1064 nm. In contrast, in the picosecond regime it is possible to remove the oxide layer on any of the three oxides at the wavelength of 355 nm. And for IR wavelengths, the maximum pulse fluence values used did not produce damage to the silicon substrate. In summary, excluding the 532 nm picosecond pulses for WOx, all laser systems allow the removal of VOx, WOx, and MoOx films without damaging the substrate. With ns pulses, the oxide layers show similar behaviour for a given wavelength, with higher threshold values at 1064 nm. With ps pulses, slightly lower fluence values are needed, since short pulses prevent thermal diffusion and energy dissipation.

Table 2. Parametric windows of the oxide removal process for ns and ps pulses at 355 nm, 532 nm, and 1064 nm.

		Parametric Window (J/cm^2)		
		355 nm	**532 nm**	**1064 nm**
WOx	**ns-pulsed**	0.17 – 1.87	0.13 – 1.98	4.93 – 10.36
	ps-pulsed	0.09 – 0.64	0.19 – 0.19	0.65 – > 1.48
VOx	**ns-pulsed**	0.13 – 2.65	0.43 – 1.59	5.39 – 9.53
	ps-pulsed	0.04 – 0.58	0.14 – >2.00	0.73 – > 1.48
MoOx	**ns-pulsed**	0.16 – 2.00	0.29 – 1.72	4.57 – 9.33
	ps-pulsed	0.06 – 0.45	0.17 – 0.38	0.51 – > 1.48

Finally, the viability of this process has been studied in the patterning of diodes using the laser source emitting at 532 nm in the ns regime, a system whose craters show good morphology and a wide parametric window for the three oxides studied. The overlap between adjacent laser pulses was parametrized. An adequate overlap leads to homogeneous and continuous laser scribes, 20-30 nm wide, with no damage to the substrate. Figure 5 shows a MoOx diode that has been isolated by a laser process at 0.25 mm from the contact edge.

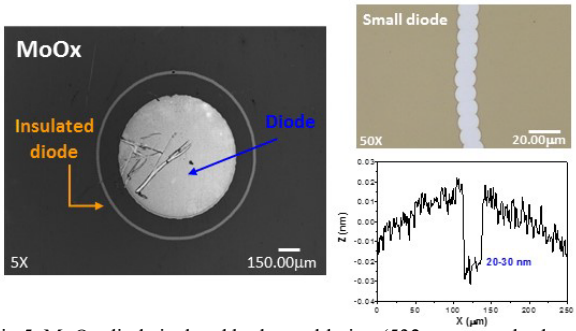

Fig.5. MoOx diode isolated by laser ablation (532 nm, ns-pulsed regime) (left). Profile of ablated spot on the MoOx film (right).

It has been reported that the high work function of transition metal oxides induces an inversion layer on the c-Si surface, with a leakage current spreading in the region surrounding the metal contact [13]. This parasitic effect can be minimized by isolating the active zone by laser ablation. Figure 6 shows the electrical characteristics of diodes before and after the laser isolation process. A remarkable improvement is observed in all cases, with a reduction of the reverse current density by two orders of magnitude. The methodology developed here could be applied to define more complex patterns, such as interdigitated contacts or planar device architectures. Note that the properties of transition metal oxides can be altered by solvents or in the thermal steps used for conventional lithography.

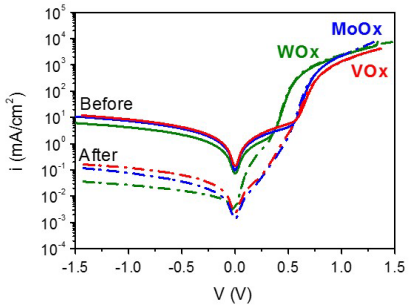

Fig. 6. Dark JV curves for oxide diodes before and after isolation.

4. Conclusions

In summary, we have studied the laser ablation of three different oxides -WOx, VOx, and MoOx, deposited by means of evaporation on silicon – with laser pulses in the nanosecond and picosecond regimes, and three different wavelengths: 355 nm, 532 nm, and 1064 nm. Regardless of the wavelength and the regime used, the ablative behaviour of the three oxides under laser irradiation in the different conditions is quite similar. It is observed that the longer wavelength induces rougher crater edges, while the shorter wavelength produces a clean edge. In order to have no substrate damage, it seems that the best choice is to use laser sources in the nanosecond regime, where the set of parameter values leading to good oxide film removal is larger. In addition to using the ns regime, it has been observed that the short wavelengths, UV and VIS, produce a lower thermal effect. The isolation of the diodes in ns pulsed at 532 nm resulted in homogeneous and continuous laser grooves, obtaining a reduction of up to two orders of magnitude in the reverse current density for the three different oxides.

Acknowledgments

Partial financial support has been provided by the Spanish Ministry of Science and Innovation under the projects CHENOC (ENE2016–78933-C4–1-R and ENE2016–78933-C4–4-R) and SCALED (PID2019–109215RB-C41 and PID2019–109215RB-C44).

References

[1] Y. Hamakawa, K. Fujimoto, K. Okuda, Y. Kashima, S. Nonomura, and H. Okamoto, ‘New types of high-efficiency solar cells based on a-Si’, *Appl. Phys. Lett.*, vol. 43, no. 7, pp. 644–646, 1983, DOI: 10.1063/1.94462.

[2] M. Taguchi, ‘Improvement of the conversion efficiency of polycrystalline silicon thin film solar cell’, *Tech. Dig. Fifth Int. Photovolt. Sci. Eng. Conf.*, pp. 689–692, 1990.

[3] A. Descoeudres *et al.*, ‘Improved amorphous/crystalline silicon interface passivation by hydrogen plasma treatment’, *Appl. Phys. Lett.*, vol. 99, no. 12, Sep. 2011, DOI: 10.1063/1.3641899.

[4] F. Feldmann, M. Bivour, C. Reichel, M. Hermle, and S. W. Glunz, ‘Passivated rear contacts for high-efficiency n-type Si solar cells providing high interface passivation quality and excellent transport characteristics’, *Sol. Energy Mater. Sol. Cells*, vol. 120, no. PART A, pp. 270–274, 2014, doi: 10.1016/j.solmat.2013.09.017.

[5] J. Meyer, S., M. Kröger, W. Kowalsky, T. Riedl, and A. Kahn, ‘Transition metal oxides for organic electronics: Energetics, device physics, and applications, *Advanced Materials*, vol. 24, no. 40. pp. 5408–5427, Oct. 23, 2012, DOI: 10.1002/adma.201201630.

[6] C. Battaglia *et al.*, ‘Silicon heterojunction solar cell with passivated hole selective MoO x contact’, *Appl. Phys. Lett.*, vol. 104, no. 11, Mar. 2014, DOI: 10.1063/1.4868880.

[7] F. Feldmann *et al.*, ‘High and Low Work Function Materials for Passivated Contacts’, in *Energy Procedia*, 2015,vol.77,pp.263–270, doi:10.1016/j.egypro.2015.07.037.

[8] L. G. Gerling *et al.*, ‘Transition metal oxides as hole-selective contacts in silicon heterojunctions solar cells’, *Sol. Energy Mater. Sol. Cells*, vol. 145, pp. 109–115, Feb. 2016, DOI: 10.1016/j.solmat.2015.08.028.

[9] S. Rung, A. Christiansen, and R. Hellmann, “Influence of film thickness on laser ablation threshold of transparent conducting oxide thin-films,” *Appl. Surf. Sci.*, vol. 305, pp. 347–351, 2014.

[10] S. Hermann, N. P. Harder, R. Brendel, D. Herzog, and H. Haferkamp, ‘Picosecond laser ablation of SiO2layers on silicon substrates, *Appl. Phys. A Mater. Sci. Process.*, vol. 99, no. 1,pp. 151–158, 2010, DOI: 10.1007/s00339-009-5464-z.

[11] L. Torrisi, A. Borrelli, and D. Margarone, ‘Study on the ablation threshold induced by pulsed lasers at different wavelengths’, *Nucl. Instruments Methods Phys. Res. Sect. B Beam Interact. with Mater. Atoms*, vol. 255, no. 2, pp. 373–379, 2007, DOI: 10.1016/j.nimb.2006.12.144.

[12] J. M. Liu, ‘Simple technique for measurements of pulsed Gaussian-beam spot sizes’, *Opt. Lett.*, vol. 7, no. 5, p. 196, 1982, DOI: 10.1364/ol.7.000196.

[13] J. Bullock, A. Cuevas, T. Allen, and C. Battaglia, “Molybdenum oxide MoOx : A versatile hole contact for silicon solar cells,” *Appl. Phys.Lett.*,vol.105,no.23,p. 232109, Dec. 2014.